Plant mediated synthesis of silver nanoparticles using Alcea rosea leaf aqueous extract and evaluation of the biological activities

Indra Ojha
ojhaindra2020@gmail.com

Far Western University

Prem Singh Saud
Far Western University

Dipak Raj Jaishi
Tribhuvan University

Yagya Raj Rosyara
Jeonbuk National University

Nepal Rama Devi
Far Western University

Prem Raj Joshi
Tribhuvan University

Hem Raj Pant
Far Western University

Article

Keywords: Alcea rosea, Ag NPs, Antioxidant, Antimicrobial, Anticancer activity

Posted Date: October 14th, 2025

DOI: https://doi.org/10.21203/rs.3.rs-7632719/v1

Additional Declarations: No competing interests reported.

Version of Record: A version of this preprint was published at Scientific Reports on January 30th, 2026. See the published version at https://doi.org/10.1038/s41598-026-37480-4.

Plant mediated synthesis of silver nanoparticles using *Alcea rosea* leaf aqueous extract and evaluation of the biological activities

Indra Ojha[1*], Prem Singh Saud[1*], Dipak Raj Jaishi[2], Yagya Raj Rosyara[3], Nepal Rama Devi[4], Prem Raj Joshi[5], and Hem Raj Pant[6]

[1]Department of Chemistry, Kailali Multiple Campus, Far Western University, Dhangadhi, Nepal

[2]Central Department of Chemistry, Tribhuvan University, Kathmandu, Nepal

[3]Department of Nano Convergence Engineering, Jeonbuk National University, 54896 Jeonju, Republic of Korea

[4]Department of Physics, Kailali Multiple Campus, Far Western University, Dhangadhi, Nepal

[5] Department of Physics, Tribhuvan University

[6]Department of Science, Far Western University, Kanchanpur, Nepal

Correspondence: premsingh@fwu.edu.np

Abstract

Silver nanoparticles (Ag NPs) are well-known for their distinctive optical, electronic, and antimicrobial properties, enabling their versatile applications in areas such as biosensors, photonics, electronics, drug delivery, and antimicrobial treatments. The biological synthesis approach offers a sustainable and eco-friendly alternative to traditional physical and chemical methods. Metal and metal oxide nanoparticles derived from plant extracts are emerging as promising agents with notable medicinal potential. This study presents a cost-effective, simple, and eco-friendly method for synthesizing silver nanoparticles (Ag NPs). This method reduces silver ions into stable Ag NPs using an aqueous leaf extract of *Alcea rosea*. The synthesized Ag NPs were characterized using various techniques, including UV-visible, FTIR, XRD, FESEM, and EDX. The Ag NPs demonstrated notable antioxidant, antimicrobial, and anticancer properties. They exhibited excellent inhibition of DPPH free radical scavenging activity, with an IC_{50} value of 80.05 ± 1.53 μg/mL. Strong antibacterial activity was observed against gram-positive *Staphylococcus aureus* and gram-negative *Shigella sonnei*, with significant MIC and MBC values. Furthermore, the nanoparticles showed potent anticancer activity, with an IC_{50} of 54.46 ± 1.67 μg/mL against cervical cancer cell lines. These findings suggest that the synthesized Ag NPs have promising potential for medical applications, especially in drug development.

Keywords: *Alcea rosea*, Ag NPs, Antioxidant, Antimicrobial, Anticancer activity

1. Introduction

Nanotechnology is one of the remarkable fields of science that focuses on the creation, synthesis, and manipulation of particles ranging in size from approximately 1 to 100 nm [1]. Nowadays, noble metal nanoparticles have gained significant attention due to their unique optical, electrical, mechanical, magnetic, and chemical properties, which distinguish them from their bulk counterparts [2]. These distinct characteristics are largely attributed to their large surface area and small size. As a result, metallic nanoparticles have found a wide range of applications across various fields, including electronics, photonics, and catalysis [3]. Various types of nanoparticles, such as copper, iron, titanium dioxide, cadmium sulfide, silver, gold, zinc, and others, exhibit unique physicochemical properties [4]. Among them, silver nanoparticles (Ag NPs) have attracted considerable interest due to their wide range of applications and diverse characteristics, including optical and magnetic polarizability [5], electrical conductivity [6], catalytic efficiency [7], antibacterial activity [8], and use in DNA sequencing [9]. Several methods have been developed for the synthesis of silver nanoparticles, including chemical, microwave-assisted, and electrochemical techniques. However, many of these approaches involve high energy consumption and the use of toxic chemicals, making purification processes challenging. To address these limitations, eco-friendly methods have been developed by incorporating biological principles into the synthesis process [10]. Green synthesis of silver nanoparticles utilizes environmentally benign reducing and capping agents, such as sugars, polysaccharides, alkaloids, and flavonoids naturally present in plant extracts [11].

Alcea rosea, commonly known as hollyhock, is a popular ornamental plant from the Malvaceae family, known for its large, vibrant flowers in a variety of colours. It is believed to have originated in the tropical regions of Southeast Asia or China. Numerous pharmacological studies have demonstrated its analgesic, antimicrobial, and anti-inflammatory properties [12]. In Iranian traditional medicine, the roots of *Alcea rosea* have been used to treat various ailments, including bronchitis, diarrhoea, constipation, inflammation, severe coughing [13]. Ethnobotanical and ethnopharmacological research on different *Alcea* species suggest their potential in treating a wide range of diseases. In herbal medicine, *A. rosea* is also used for managing snake bites, jaundice, malaria, rheumatism, renal and urinary tract infections, as well as digestive disorders accompanied by vomiting and diarrhoea [14].

Various plant extracts, such as those from *Dalbergia spinosa*, *Buddleja globosa*, and *Argemone mexicana*, have been reported in the literature for the green synthesis of silver nanoparticles (Ag NPs). In this study, *Alcea rosea* leaf extract was used to synthesize silver nanoparticles, which were characterized using UV–Visible spectroscopy, FTIR, XRD, FESEM, and EDX analyses. Furthermore, the anticancer, antioxidant, and antibacterial properties of the synthesized nanoparticles were investigated [15-17]. To the best of our knowledge, limited information is available on the manufacture of silver nanoparticles (Ag NPs) utilizing *Alcea rosea* leaf extract. To the best of my knowledge, this research may be the first report on the synthesis of silver nanoparticles using *Alcea rosea* leaf extract for various biological applications.

The major active phytochemical compounds present in this medicinal plant are illustrated in **Figure 1**.

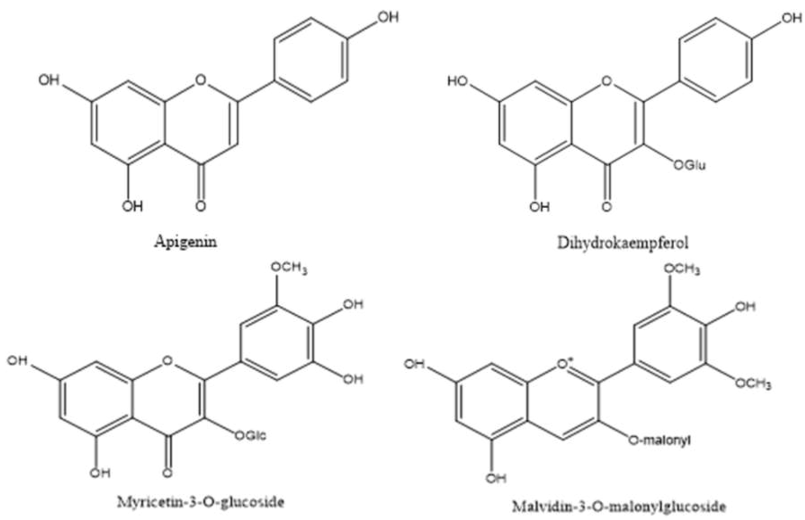

Fig 1: Major active chemical compounds reported from *Alcea rosea.*

2. Materials and Methods

2.1 Chemicals and instruments

The glassware used in this study was made from Type 1 Class borosilicate glass and included beakers, funnels, test tubes, Falcon tubes, volumetric flasks, 96-well microdilution plates, and conical flasks. The equipment utilized comprised a microplate reader (Epoch 2, Biotek Instruments, Inc., USA), a water bath (Clifton), a hot air oven (Griffin-Grundy), and a pH meter. Mueller Hinton Broth (MHB), neomycin, and Resazurin were supplied by HiMedia (LOBA CHEMI Pvt. Ltd), while Nutrient Agar (NA) was also used. Various chemicals and reagents employed in the bioassays included methanol, quercetin, ascorbic acid, and DPPH reagents, all procured from Merck and Sigma. Additionally, MTT reagent and LB powder (Sisco Research Laboratories Pvt. Ltd, India) were among other reagents used in this study.

2.2 Plant sample collection and preparation of aqueous extract

Alcea rosea was collected from the Kailali district, Nepal, on February 15, 2025. The coordinates of the collection site are 28° 49′ N and 80° 53′ E. After collection, the plant material was carefully cleaned, shade-dried, and finely powdered using a grinding mixture. Approximately 20 grams of the powder was dissolved in 200 mL of distilled water in a beaker. The mixture was then heated to 50°C for one hour and stirred using a hot magnetic stirrer. The solution was then filtered using Whatman No. 1 filter paper, and the filtrate was then stored for later use at 4°C [18].

2.3 Plant mediated synthesis of silver nanoparticles

A 100 mL solution of $AgNO_3$ (1 mM) was mixed with 5 mL of aqueous plant extract and heated on a magnetic stirrer-equipped hot plate for 20 minutes. The mixture was then stirred at room temperature for approximately one hour, with the pH adjusted to an optimal value of 11. A colour shift of the reaction mixture from pale yellow or brown to deep brown indicated the formation of silver nanoparticles. The synthesis of silver nanoparticles was confirmed by UV-visible spectrophotometry, which detected surface plasmon resonance (SPR) with an absorbance peak between 300 and 600 nm [19].

2.4 Antioxidant activity

The antioxidant activity of the nanoparticles was evaluated using the 2,2-diphenyl-1-picrylhydrazyl (DPPH) assay, with slight modification to previously reported protocols where we assessed the ability of nanoparticles to suppress free radicals [20]. The antioxidant activity was measured using a 96-well plate reader that was modified from the colorimetric method. Each of the 96-well plates received 100 µL solution of nanoparticles. At 517 nm, the initial reading was recorded. Next, 100 microliters of DPPH were added to each 96-well plate. The final measurement at 517 nm was recorded using a microplate reader. The IC_{50} value was calculated by using software called GraphPad Prism.

Radical scavenging ability = $Abs_{control}$ - Abs_{sample} / $Abs_{control}$ × 100 %……...(i)

Where, $A_{control}$ = absorbance of the control, and A_{sample} = absorbance of the sample

2.5 Antibacterial Assay

The agar well diffusion assay, with minor modifications, was used to evaluate the antibacterial activity [21]. Mueller-Hinton broth (MHB) was used for bacterial culture, where commercially available Mueller-Hinton agar (MHA) was dissolved in distilled water, steamed, autoclaved, poured into sterile Petri plates, and then left to solidify. After the agar had solidified, different bacterial strains were inoculated onto the plates, and their concentrations were adjusted according to the McFarland standard. Wells were carefully drilled into the agar, and the test samples were added to the well, along with a positive control (neomycin) and a negative control (50% DMSO). The inoculated petri plates were kept in an incubator for 18 to 24 hours, and the zone of inhibition (ZOI) was measured using a scale.

2.6 Resazurin microtiter assay

The minimum inhibitory concentration (MIC) and minimum bactericidal concentration (MBC) of nanoparticles were calculated by the use of resazurin microtiter test [22]. The test organisms were Gram-negative *Shigella sonnei* and Gram-positive *Staphylococcus aureus*. In a 96-well microtiter plate, 100 µL of double-strength Mueller-Hinton broth (MHB) was added to each well, followed by 100 µL of the nanoparticle sample solution in the first row. Serial two-fold dilutions (ranging from 50 to 0.390 mg/mL) were performed from rows A to H using a multichannel micropipette. Each well received 10 µL of bacterial culture (0.5 McFarland standard) and was incubated for 24 hours at 37 °C. Afterward, 5 µL of 0.3% resazurin was added, and the plate was incubated for another two hours. The lowest nanoparticle concentration showing pink colour was recorded as MIC. Finally, 50 µL solutions were added to Mueller-Hinton broth agar plates to determine the MBC of the sample.

2.7 MTT assay

Cytotoxicity of the silver nanoparticles (Ag NPs) was evaluated against cervical cancer (HeLa) and lung cancer (A549) cell lines using the MTT assay [23]. Dulbecco's Modified Eagle Medium (DMEM) was used to seed 10^4 cells/well in a 96-well plate, which was incubated for 48 hours at 37 °C with 5% CO_2. After the incubation, different concentrations of Ag NPs (400 to 50 µg/mL) were added, followed by another 48-hour incubation. Following treatment, the supernatant was carefully removed, and 100 µL of fresh DMEM, along with 20 µL of MTT solution (5 mg/mL), was added to each well. After 4 hours of incubation, purple formazan crystals were observed. These were subsequently dissolved by adding 100 µL of 0.1% DMSO per well and incubating for 15 minutes at room temperature. Absorbance was measured at 570 nm using a microplate reader.

The percentage of cytotoxicity was calculated using the following formula:

% cytotoxic activity = $Abs_{control}$ - Abs_{sample} / $Abs_{control}$ × 100 %……...(i)

Where $A_{control =}$ is the control's absorbance, and A_{sample} is the treated sample's absorbance.

2.8 Characterization of silver nanoparticles

2.8.1 UV-Visible spectroscopy

A noticeable change was noted in the colour of the solution as it became brownish, indicating the formation. The presence of silver nanoparticles was confirmed preliminarily, as the UV-vis absorption was seen in the 300-600 nm region. It was measured employing a UV spectrophotometer [SPECORD 200 PLUS, (An Endress+Hauser Company)].

2.8.2 FTIR spectroscopy

FTIR spectroscopy (PerkinElmer UV/VIS Lambda 365 Spectrophotometer) was used to analyze the phytochemicals adsorbed onto the nanoparticles, as well as the organic functional groups present in the aqueous extract, within the wavenumber range of 400–4000 cm^{-1}. The characteristic IR peaks at specific wave numbers indicate the participation of these compounds in the synthesis and stabilization of the metal nanoparticles.

2.8.3 XRD analysis

The crystallographic structure, grain size, and diffraction pattern of the synthesized silver nanoparticles (Ag NPs) were characterized using X-ray diffraction (XRD) analysis (D2 Phaser, Bruker, NAST, Nepal) operated at 30 kV with a Cu Kα radiation wavelength of 1.54 Å. The diffraction data were collected over a 2θ range of 20° to 80°. The average crystallite size of the nanoparticles was calculated using the Scherrer equation.

2.8.4 FESEM analysis

Field emission scanning electron microscopy (FE-SEM) (SU equipment, Korea) was employed to examine the surface morphology, grain size, and other physical properties of the synthesized nanoparticles. The particle sizes were quantified using ImageJ software

2.8.5 EDX analysis

The elemental composition of the produced Ag nanoparticles was examined using this technique.

Statistical Analysis

The results of the triplicate tests were displayed as mean ± standard deviation. GraphPad Prism was used to calculate the IC_{50} and create accompanying graphs for the DPPH and MTT assays. FTIR, XRD, and UV-visible spectra were plotted using Origin. ImageJ software was used to analyze SEM images.

3. Results and Discussion

Nanoparticles are excellent tools for science and study because of their vast surface area and high activity. Green-synthesized silver nanoparticles are useful materials that have been explored for addressing a number of modern biological, industrial, and environmental issues. A variety of methods, including UV-vis, FTIR, XRD, SEM, and EDX, were used to characterize these nanoparticles, which were synthesized from the aqueous extract of *A. rosea*. The synthesized nanoparticles tested for different applications, including antimicrobial, antioxidant mitigation, and cancer treatment. Various sections deal with extensive discussions.

3.1 UV-vis spectroscopy

UV–visible spectroscopy is recognized as a vital analytical method, effectively serving as both a qualitative and quantitative approach. It is a rapid and preliminary technique used to confirm the successful synthesis of nanoparticles derived from plant extracts. The phytochemicals in plant extracts serve as reducing agents, converting metal ions into nanoparticles and aiding in their formation, stabilization, and surface capping. The biosynthesized silver nanoparticles (Ag NPs) demonstrated a peak absorption at 411 nm, consistent with findings from previous studies [24]. This absorption behaviour arises from the excitation of electrons from the valence band to the conduction band, leading to surface plasmon resonance (SPR) [25. Typically, silver nanoparticles (Ag NPs) exhibit a distinct surface plasmon resonance (SPR) peak in the range of 400 to 450 nm, confirming their successful formation [26]. The UV-Vis absorption spectrum of the synthesized nanoparticles is shown in Figure 2.

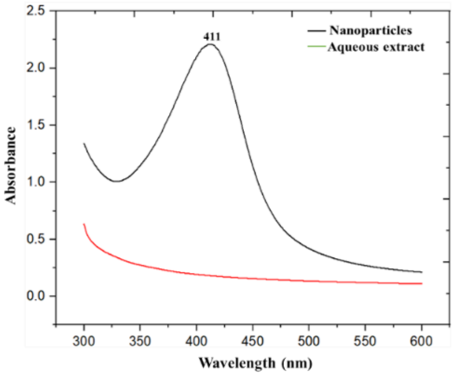

Figure 2: UV spectra of Ag NPs and aqueous extract.

3.2 Fourier transform infrared spectroscopy (FTIR)

FTIR spectroscopy studies were performed on the synthesized nanoparticles and their aqueous extract. The changes in peak positions and intensities between the FTIR spectra of the nanoparticles and aqueous extract have confirmed the involvement of plant secondary metabolites in the synthesis of nanoparticles. An IR peak at 3670 cm^{-1} is generally indicative of (O-H) group, particularly a free or weakly hydrogen-bonded O-H stretching, and may be connected to alcoholic and phenolic substances. The vibrational peaks around 3359 cm^{-1} most likely is due to the O-H stretching vibration of an alcohol or carboxylic acid, or potentially the N-H stretching vibration of an amine. The C-H stretching vibration is visible in the peak projected at 2914 cm^{-1}. The stretching of the C-N group is responsible for the peak at about 1061 cm^{-1}, whereas the stretching of the C-H group is responsible for the peak at 1403 cm^{-1}. The FTIR spectra detected a characteristic peak at about 506 cm^{-1}, which might have been caused by the stretching of the Ag nanostructure [27]. The FTIR analysis results suggest that these peaks are consistent with earlier findings, indicating a promising correlation that supports our research [28]. **Figure 3** displays the FTIR spectra of the synthesized Ag NPs and aqueous extract.

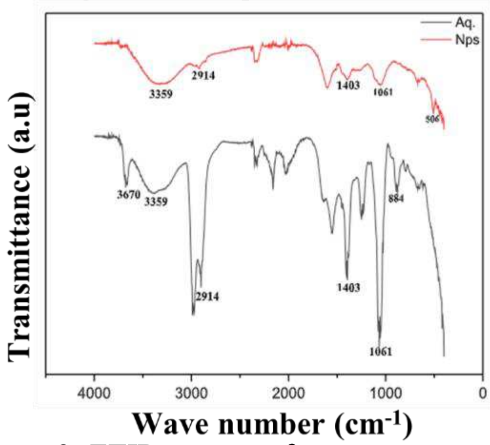

Figure 3: FTIR spectra of aqueous extract and synthesized Ag NPs.

3.3 XRD analysis

XRD is a special method that gives an abundance of information regarding the crystalline characteristics of nanoparticles. Debye-Scherrer's equation can be used to determine the average crystallographic size based on the most intense XRD diffraction peak.

$$D = \frac{K\lambda}{\beta \mathrm{Cos}\theta}$$

Where, θ is Bragg's diffraction angle, β is the full width at half maximum (FWHM) of the most intense peak, expressed in radians, and λ is the X-ray wavelength, which has a value of 0.15406 Aº [29-31]. Using Debye-Scherrer's equation, the average crystalline size was 5.38 nm. The diffraction peaks observed at 38.3º, 44.6º, 68.8º, and 77.6º correspond to (111), (200), (220), and (311) planes of face-centred cubic (FCC) crystal structure (JCPDS card 04-0783) [32]. The obtained XRD data are consistent with the previously published studies that validate the cubic structure of silver nanoparticles [33-34]. Comparable XRD patterns were found in *Erigeron bonariensis* [35] and *Alternaria solani* [36]. SEM images are valuable for providing insights into molecular structures, whereas XRD is effective in determining grain size. This distinction highlights the unique strengths of each technique and the complementary information they offer in material analysis [37]. **Figure 4** displays XRD spectra of the synthesized Ag NPs.

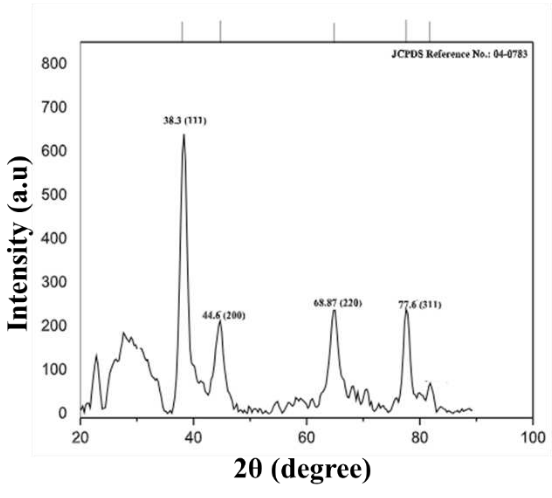

Fig 4: XRD spectra of Ag NPs.

3.4 FESEM analysis

Morphological size and shape of Ag NPs produced by the aqueous extract of *A. rosea* were analyzed through the FE-SEM. Synthesized Ag NPs were predominantly spherical with a diameter ranging from 22 to 64 nm and an average particle size of 35.37 nm at a 500 nm scale. In the UV-visible spectra of biosynthesized Ag NPs, a single SPR peak indicates the formation of spherical particles, which is further confirmed by the SEM image [38]. There have been reports of the biosynthesis of spherical and smooth nanoparticles in *Rheum emodi* [39] and honey-mediated green synthesis of silver nanoparticles [40]. The electrostatic interaction and hydrogen bonding between the bioinorganic capping molecules attached to the silver nanoparticles assist in the development of the SEM image. It is shown that uniform, fairly spherical silver nanoparticles were produced. Even inside the aggregates, there was no direct contact between the nanoparticles, suggesting that a capping agent had stabilized them [41]. The particle size is displayed in **Figure 5** at various resolutions from the FE-SEM picture.

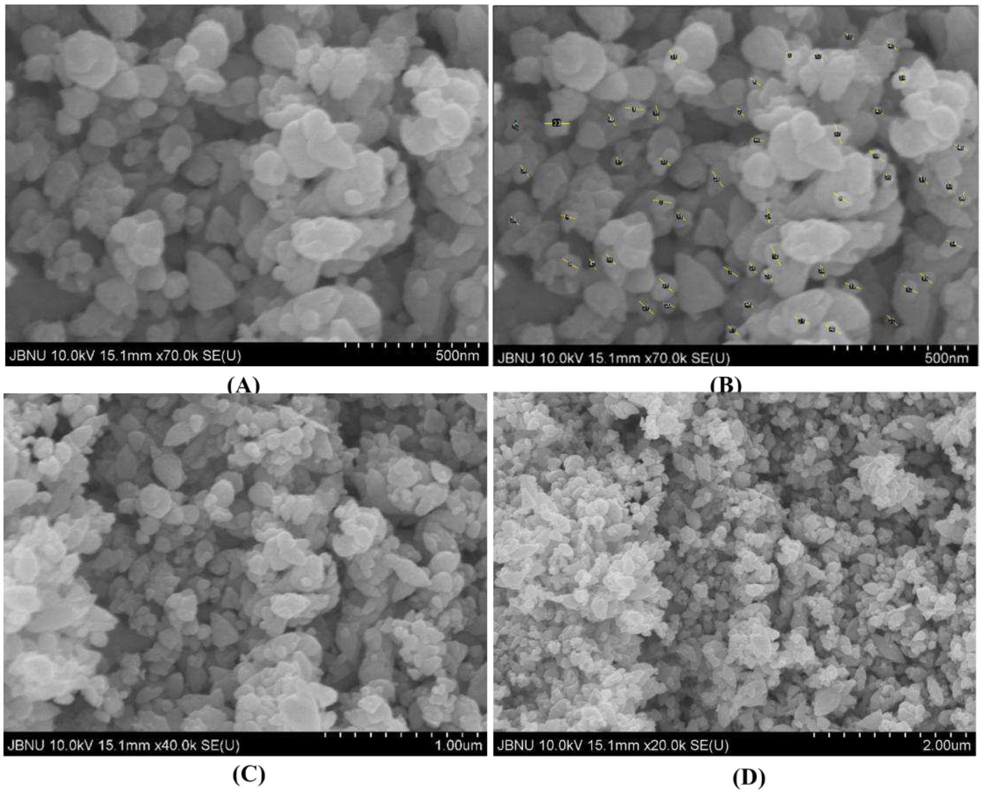

Fig 5: Synthesized nanoparticles captured FE-SEM images (a) 500 nm scale, (b) length measurement of Ag NPs, (c) Scale: 1 µm, (d) Scale: 2 µm.

3.5 EDX analysis

Elemental mapping of the synthesized silver nanoparticles is presented in **Figure 6**. In the elemental mapping image, the yellow-coloured spots correspond to the distribution of silver nanoparticles across the sample surface.

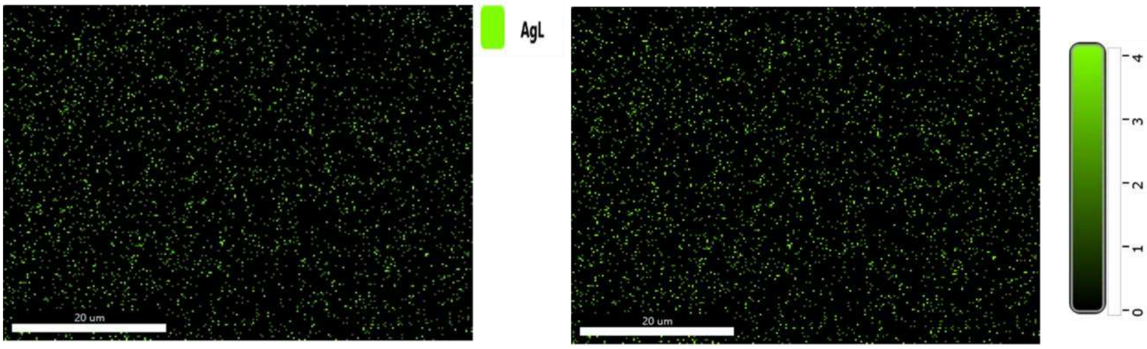

Figure 6: EDX images indicating the Ag element.

Application of biosynthesized Ag nanomaterials

3.6 Antioxidant potential

The antioxidant potential of the synthesized silver nanoparticles was evaluated using the DPPH assay. DPPH possesses hydrogen-accepting properties that make it useful for evaluating antioxidant activity. It readily accepts electrons from antioxidant compounds, leading to a color change from violet to yellow. Through this process, the DPPH free radical is reduced to a stable diamagnetic molecule. In this study, the DPPH radical scavenging activity of Ag NPs increased with rising concentrations, reaching its maximum at higher levels. The biosynthesized Ag NPs achieved an IC_{50} value of 80.05 ± 1.53 µg/mL, compared to 3.55 ± 1.61 µg/mL for quercetin. When synthesized using leaf extract, the nanoparticles demonstrated slightly lower antioxidant activity than that reported in earlier studies [42]. The presence of hydroxyl groups in flavonoids likely contributes to nanoparticle stabilization and imparts additional bioactivities. The observed antioxidant effect may arise from mechanisms such as single-electron transfer, hydrogen donation, or metal ion chelation [43].

Table 1: Antioxidant potential (IC_{50}) values of synthesized nanoparticles and standard quercetin.

Samples	IC_{50} (µg/mL)
Ag NPs	80.05 ± 1.53
Quercetin	3.55 ± 1.61

3.7 In vitro antibacterial potential

3.7.1 Agar well diffusion method

Both *S. aureus* and *S. sonnei* exhibited inhibition zones of 13 mm, while *K. pneumoniae* and *E. coli* showed zones of 8 mm each. These findings are consistent with previous studies reporting the antibacterial efficacy of Ag NPs [44, 45]. The antimicrobial activity is attributed to the combined effects of Ag^{+} ions and the membrane-disrupting action of the polymeric components. Green-synthesized Ag NPs demonstrate strong bactericidal potential, particularly against drug-resistant strains, making them promising candidates for biomedical applications [46]. The corresponding inhibition zones and representative antibacterial petri plate images are presented in **Table 2** and **Figure 7**.

Table 2: Zone of inhibition shown by silver nanoparticles against the test organisms.

Sample	Bacteria	ZOI sample (mm)	ZOI positive control (neomycin) (mm)
Ag NPs	*S. aureus*	13	21
	S. sonnei	13	20
	K pneumoniae	8	20
	E. coli	8	20

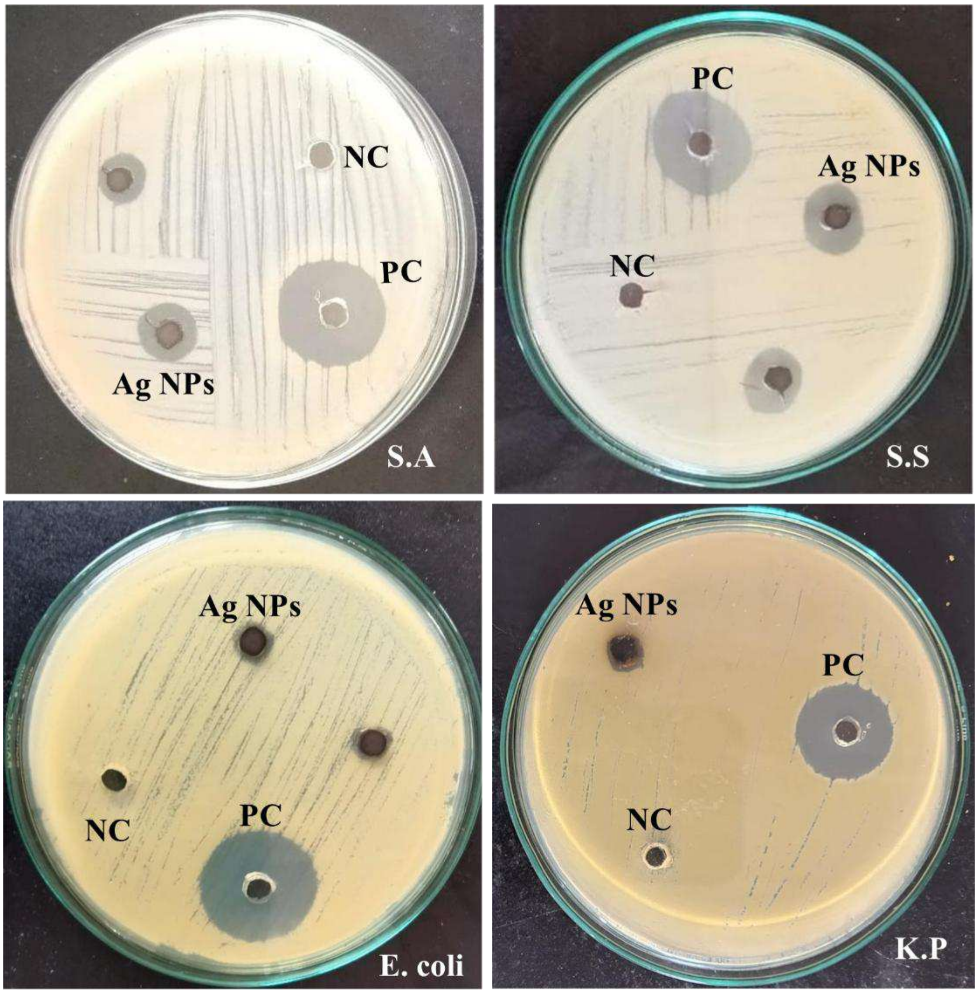

Fig 7: Antibacterial test slides against different bacterial strains.

3.7.2 MIC and MBC

The MIC and MBC of the nanoparticles against the Gram-negative *S. sonnei* and the Gram-positive *S. aureus* were determined using the resazurin microtiter assay. Resazurin, a blue dye, is reduced by the NADH dehydrogenase enzyme in metabolically active cells to produce resorufin, a pink-coloured compound. Since this enzyme is only present in viable cells, the assay serves as an effective method for assessing cell viability [47]. MIC and MBC of nanoparticles against *S. aureus* and *S. sonnei* are shown in **Table 3**; they are 6.25 mg/mL and 12.5 mg/mL, respectively. Ag NPs synthesized from *Pogonatherum crinitum* leaf extracts demonstrated comparable MIC and MBC values, according to the literature [48]. The MIC and MBC of the positive control neomycin against *S. aureus* and *S. sonnei* were found to be 0.78 and 1.56 mg/mL, respectively.

Table 3: MIC and MBC values for nanoparticles.

Samples	*Staphylococcus aureus*		*Shigella sonnei*	
	MIC (mg/mL)	MBC (mg/mL)	MIC (mg/mL)	MBC (mg/mL)
Ag NPs	6.25	12.5	6.25	12.5
Neomycin	0.78	1.56	0.78	1.56

3.8 Cytotoxicity

The anticancer activity of biosynthesized Ag NPs against A549 and HeLa cancer cells was evaluated by measuring the cellular reduction of MTT, as determined by in vitro examination. Ag NPs at varying concentrations (400-50 μg/mL) were applied to both cancer cells over 48 hours, causing a dose-dependent inhibition of the cancer cells. Based on our findings, silver nanoparticles show significant anticancer potential. As the concentration of Ag NPs decreased, their anticancer capability also reduced. The results showed a dose-dependent inhibition, with the greatest inhibition being 39.37% for A549 and 49.07% for HeLa cell mortality at 400 μg/mL. The calculated IC_{50} values for A549 and HeLa were 54.46 ± 1.67 μg/mL and 92.93 ± 1.05 μg/mL, respectively, confirming the excellent therapeutic potential of Ag NPs. These findings are consistent with earlier research on the A549 cancer cell line [49]. Mechanistically, silver nanoparticles are known to impair mitochondrial function, elevate intracellular reactive oxygen species, and induce apoptosis, thereby exerting cytotoxic effects on cancer cells. This supports the potential of Ag NPs as promising candidates for cancer treatment [50].

Table 4: The IC_{50} of silver nanoparticles.

Cell lines	IC_{50} (µg/mL)
Lung cancer A549	54.46 ± 1.67
HeLa	92.93 ± 1.05

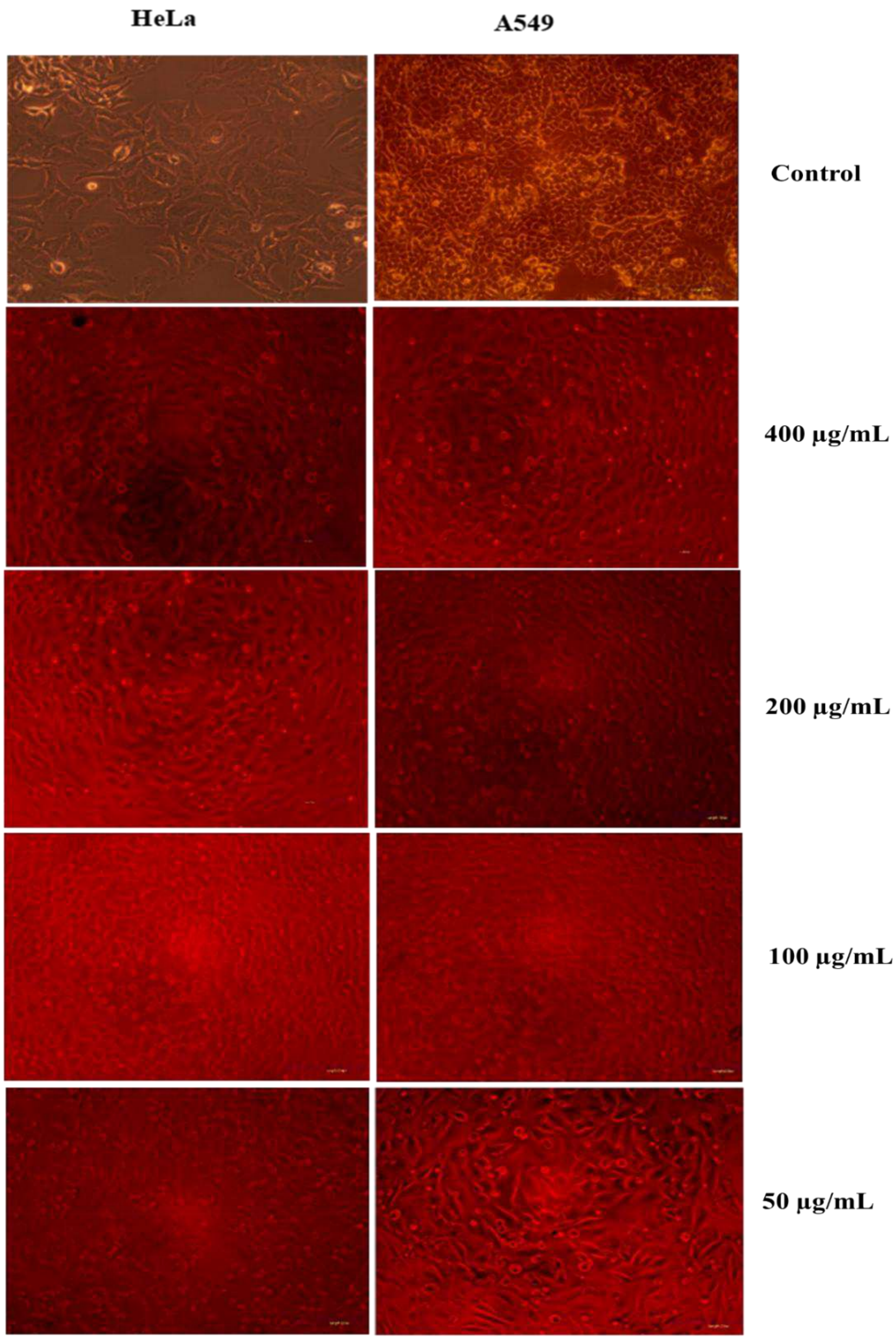

Fig 8: The photographs showing HeLa and A549 cells before and after treatment with Ag NPs at different concentrations.

4. Conclusion

In conclusion, we report a simple, cheaper, and biologically inspired approach for synthesizing silver nanoparticles (Ag NPs) using an aqueous extract of *Alcea rosea.* The successful formation of Ag NPs was confirmed through various techniques, including UV-vis spectroscopy, FTIR, XRD, FE-SEM, and EDX analysis. The biosynthesized Ag NPs exhibited potent antibacterial activity against *Staphylococcus aureus* and *Shigella sonnei*, with notable minimum inhibitory concentration (MIC) and minimum bactericidal concentration (MBC) values observed for both strains. Moreover, the synthesized Ag NPs exhibited superior antioxidant activity. Biogenic Ag NPs also demonstrated notable anticancer effects against both tested cell lines. These findings suggest that the *A. rosea-mediated* green synthesis technique produces high-quality silver nanoparticles with promising multifunctional biomedical applications. This process offers a safer and more sustainable alternative for disease treatment and management. This study highlights the potential of plant-derived secondary metabolites in the eco-friendly synthesis of metal nanoparticles and underscores the significance of Nepalese medicinal plants as valuable resources for advancing nanotechnology.

Author contributions

Indra Ojha: Methodology, formal analysis, writing-original draft, review and editing, **Prem Singh Saud:** Data curation, modification, review supervision, and conceptualization, **Dipak Raj Jaishi:** Composing and revising, **Yagya Raj Rosyara:** Writing and editing, **Nepal Rama Devi:** Composing and formal evaluation, **Prem Raj Joshi:** Writing and reviewing, **Hem Raj Pant:** Writing, review, editing, supervision, and conceptualization.

Acknowledgments

We are grateful to the Department of Science, Kailali Multiple Campus, Far Western University, for providing laboratory facilities. For XRD data acquisition, we sincerely thank the Nepal Academy of Science and Technology (NAST), Lalitpur, Nepal. We also express our heartfelt appreciation to Jeonbuk National University, Republic of Korea, for providing FESEM and EDX imaging support. The authors are greatly indebted to the Central Department of Chemistry, Tribhuvan University, for UV-vis, FTIR, antibacterial, antioxidant, and anticancer tests.

Competing interest

Regarding the current publication, the authors reveal no conflicts of interest.

Funding

There was no outside support for this study; it was entirely self-funded.

Data availability

Upon reasonable request, the corresponding author will provide the datasets used and/or analyzed in the current study.

Ethical approval

The study was carried out in accordance with Far-western University's institutional procedures. *A. rosea* is not included in any endangered species list or the Convention on International Trade in Endangered Species of Fauna and Flora. The Plant Protection Act and the International Plant Protection Convention were followed, and no endangered plant species were harmed or disturbed during this study. Since the study was carried out in Sudurpaschim, it met with all applicable state and federal laws.

References

[1] Luo, G.; Du, L.; Wang, Y.; Wang, K. Manipulation and Control of Structure and Size of Inorganic Nanomaterials in Microchemical Systems. *Chem. Eng. Technol*, *42* (10), 1996–2008. https://doi.org/10.1002/ceat.201900067, **2019**.

[2] Mazur, M. Electrochemically Prepared Silver Nanoflakes and Nanowires. *Electrochem. Commun*, *6* (4), 400–403. https://doi.org/10.1016/j.elecom.2004.02.011, **2004**.

[3] Khursheed, R.; Dua, K.; Vishwas, S.; Gulati, M.; Jha, N. K.; Aldhafeeri, G. M.; Alanazi, F. G.; Goh, B. H.; Gupta, G.; Paudel, K. R.; Hansbro, P. M.; Chellappan, D. K.; Singh, S. K. Biomedical Applications of Metallic Nanoparticles in Cancer: Current Status and Future Perspectives. *Biomed. Pharmacother*, *150*, 112951. https://doi.org/10.1016/j.biopha.2022.112951, **2022**.

[4] Jamkhande, P. G.; Ghule, N. W.; Bamer, A. H.; Kalaskar, M. G. Metal Nanoparticles Synthesis: An Overview on Methods of Preparation, Advantages and Disadvantages, and Applications. *J. Drug Deliv. Sci. Technol*, *53*, 101174. https://doi.org/10.1016/j.jddst.2019.101174, **2019**.

[5] Taleb, A.; Russier, V.; Courty, A.; Pileni, M. P. Collective Optical Properties of Silver Nanoparticles Organized in Two-Dimensional Superlattices. *Phys. Rev. B*, *59* (20), 13350–13358. https://doi.org/10.1103/PhysRevB.59.13350, **1999**.

[6] Alshehri, A. H.; Jakubowska, M.; Młożniak, A.; Horaczek, M.; Rudka, D.; Free, C.; Carey, J. D. Enhanced Electrical Conductivity of Silver Nanoparticles for High Frequency Electronic Applications. *ACS Appl. Mater. Interfaces* **2012**, *4* (12), 7007–7010. https://doi.org/10.1021/am3022569.

[7] Jiang, Z.-J.; Liu, C.-Y.; Sun, L.-W. Catalytic Properties of Silver Nanoparticles Supported on Silica Spheres. *J. Phys. Chem. B*, *109* (5), 1730–1735. https://doi.org/10.1021/jp046032g, **2005**.

[8] Tang, S.; Zheng, J. Antibacterial Activity of Silver Nanoparticles: Structural Effects. *Adv. Healthc. Mater*, *7* (13), 1701503. https://doi.org/10.1002/adhm.201701503, **2018**.

[9] Wu, J.; Tan, L. H.; Hwang, K.; Xing, H.; Wu, P.; Li, W.; Lu, Y. DNA Sequence-Dependent Morphological Evolution of Silver Nanoparticles and Their Optical and Hybridization Properties. *J. Am. Chem. Soc, 136* (43), 15195–15202. https://doi.org/10.1021/ja506150s, **2014**.

[10] Ravichandran, V.; Vasanthi, S.; Shalini, S.; Ali Shah, S. A.; Harish, R. Green Synthesis of Silver Nanoparticles Using Atrocarpus Altilis Leaf Extract and the Study of Their Antimicrobial and Antioxidant Activity. *Mater. Lett*, *180*, 264–267. https://doi.org/10.1016/j.matlet.2016.05.172, **2016**.

[11] Raveendran, P.; Fu, J.; Wallen, S. L. Completely "Green" Synthesis and Stabilization of Metal Nanoparticles. *J. Am. Chem. Soc, 125* (46), 13940–13941. https://doi.org/10.1021/ja029267j, **2003**.

[12] Dar, P. A.; Ali, F.; Sheikh, I. A.; Ganie, S. A.; Dar, T. A. Amelioration of Hyperglycaemia and Modulation of Antioxidant Status by *Alcea Rosea* Seeds in Alloxan-Induced Diabetic Rats. *Pharm. Biol*, *55* (1), 1849–1855. https://doi.org/10.1080/13880209.2017.1333127, **2017**.

[13] Ahmadi, M.; Rad, A.; Rajaei, Z.; Hadjzadeh, M.-A.-R.; Mohammadian, N.; Tabasi, N. Alcea Rosea Root Extract as a Preventive and Curative Agent in Ethylene Glycol-Induced Urolithiasis in Rats. *Indian J. Pharmacol*, *44* (3), 304. https://doi.org/10.4103/0253-7613.96298, **2012**.

[14] Raffi Shehzad, M.; Hanif, M. A.; Rehman, R.; Bhatti, I. A.; Hanif, A. Hollyhock. In *Medicinal Plants of South Asia*; Elsevier; pp 381–391. https://doi.org/10.1016/B978-0-08-102659-5.00029-X, **2020**.

[15] Muniyappan, N.; Nagarajan, N. S. Green Synthesis of Silver Nanoparticles with Dalbergia Spinosa Leaves and Their Applications in Biological and Catalytic Activities.

Process Biochem, *49* (6), 1054–1061. https://doi.org/10.1016/j.procbio.2014.03.015, **2014**.

[16] Carmona, E. R.; Benito, N.; Plaza, T.; Recio-Sánchez, G. Green Synthesis of Silver Nanoparticles by Using Leaf Extracts from the Endemic *Buddleja Globosa* Hope. *Green Chem. Lett. Rev*, *10* (4), 250–256. https://doi.org/10.1080/17518253.2017.1360400, **2017**.

[17] Oni, B. A.; Sanni, S. E.; Agu, K. C.; Tomomewo, O. S. Green Synthesis of Ag Nanoparticles from Argemone Mexicana L. Leaf Extract Coated with MOF-5 for the Removal of Metronidazole Antibiotics from Aqueous Solution. *J. Environ. Manage, 342*, 118161. https://doi.org/10.1016/j.jenvman.2023.118161, **2023**.

[18] Javan Bakht Dalir, S.; Djahaniani, H.; Nabati, F.; Hekmati, M. Characterization and the Evaluation of Antimicrobial Activities of Silver Nanoparticles Biosynthesized from Carya Illinoinensis Leaf Extract. *Heliyon*, *6* (3), e03624. https://doi.org/10.1016/j.heliyon.2020.e03624, **2020**.

[19] Regmi, B.; Binadi, T. R.; Jha, S. N.; Chaudhary, R. K.; Poudel, B. R.; Gautam, S. K. Antibacterial and Antioxidant Studies of Green Synthesized Silver Nanoparticles Using Azadirachta Indica (Neem) Leaf Extract. *Int. J. Appl. Sci. Biotechnol*, *9* (3), 220–226. https://doi.org/10.3126/ijasbt.v9i3.39069, **2021**.

[20] Bhandari, D. P.; Poudel, D. K.; Satyal, P.; Khadayat, K.; Dhami, S.; Aryal, D.; Chaudhary, P.; Ghimire, A.; Parajuli, N. Volatile Compounds and Antioxidant and Antimicrobial Activities of Selected Citrus Essential Oils Originated from Nepal. *Molecules*, *26* (21), 6683. https://doi.org/10.3390/molecules26216683, **2021**.

[21] Abbey, T. C.; Deak, E. What's New from the CLSI Subcommittee on Antimicrobial Susceptibility Testing M100, 29th Edition. *Clin. Microbiol. Newsl*, *41* (23), 203–209. https://doi.org/10.1016/j.clinmicnews.2019.11.002, **2019**.

[22] Sarker, S. D.; Nahar, L.; Kumarasamy, Y. Microtitre Plate-Based Antibacterial Assay Incorporating Resazurin as an Indicator of Cell Growth, and Its Application in the in Vitro Antibacterial Screening of Phytochemicals. *Methods*, *42* (4), 321–324. https://doi.org/10.1016/j.ymeth.2007.01.006, **2007**.

[23] Krishnaraj, C.; Muthukumaran, P.; Ramachandran, R.; Balakumaran, M. D.; Kalaichelvan, P. T. Acalypha Indica Linn: Biogenic Synthesis of Silver and Gold Nanoparticles and Their Cytotoxic Effects against MDA-MB-231, Human Breast Cancer Cells. *Biotechnol. Rep*, *4*, 42–49. https://doi.org/10.1016/j.btre.2014.08.002, **2014**.

[24] Tyagi, P. K.; Tyagi, S.; Gola, D.; Arya, A.; Ayatollahi, S. A.; Alshehri, M. M.; Sharifi-Rad, J. Ascorbic Acid and Polyphenols Mediated Green Synthesis of Silver Nanoparticles from Tagetes Erecta L. Aqueous Leaf Extract and Studied Their Antioxidant Properties. *J. Nanomater*, *2021*, 1–9. https://doi.org/10.1155/2021/6515419, **2021**.

[25] Barzinjy, A. A.; Haji, B. Sh. Green Synthesis and Characterization of Ag Nanoparticles Using Fresh and Dry *Portulaca Oleracea* Leaf Extracts: Enhancing Light Reflectivity Properties of ITO Glass. *Micro Nano Lett, 19* (3), e12198. https://doi.org/10.1049/mna2.12198, **2024**.

[26] Kamarudin, D.; Hashim, N. A.; Ong, B. H.; Che Hassan, C. R.; Abdul Manaf, N. Synthesis of Silver Nanoparticles Stabilised by PVP for Polymeric Membrane Application: A Comparative Study. *Mater. Technol*, *37* (5), 289–301. https://doi.org/10.1080/10667857.2021.1908768, **2022**.

[27] Barzinjy, A. A.; Haji, B. Sh. Green Synthesis and Characterization of Ag Nanoparticles Using Fresh and Dry *Portulaca Oleracea* Leaf Extracts: Enhancing Light Reflectivity Properties of ITO Glass. *Micro Nano Lett, 19* (3), e12198. https://doi.org/10.1049/mna2.12198, **2024**.

[28] Eltarahony, M.; Ibrahim, A.; El-shall, H.; Ibrahim, E.; Althobaiti, F.; Fayad, E. Antibacterial, Antifungal and Antibiofilm Activities of Silver Nanoparticles Supported by Crude Bioactive Metabolites of Bionanofactories Isolated from Lake Mariout. *Molecules*, *26* (10), 3027. https://doi.org/10.3390/molecules26103027, **2021**.

[29] Dhungana, S.; Paudel, B. R.; Gautam, S. K. Synthesis and Characterization of ZnTe Nanoparticles. *Nepal J. Sci. Technol*, *17* (1), 1–3. https://doi.org/10.3126/njst.v17i1.25054, **2016**.

[30] Regmi, A.; Bhandari, J.; Bhattarai, S.; Gautam, S. K. Synthesis, Characterizations and Antimicrobial Activity of Cuprous Oxide (Cu2O) Nanoparticles. *J. Nepal Chem. Soc, 40*, 5–10. https://doi.org/10.3126/jncs.v40i0.27271, **2019**.

[31] Gautam, S. K.; Sapkota, B.; Bhujel, A.; Bhattarai, S. Estimation of Particle Size and Band Gap of Zinc Oxide Nanoparticle Synthesized by Chemical Precipitation Method. *J. Nepal Chem. Soc*, *41* (1), 46–50. https://doi.org/10.3126/jncs.v41i1.30448, **2020**.

[32] Mehta, B. K.; Chhajlani, M.; Shrivastava, B. D. Green Synthesis of Silver Nanoparticles and Their Characterization by XRD. *J. Phys. Conf. Ser*, *836*, 012050. https://doi.org/10.1088/1742-6596/836/1/012050, **2017**.

[33] Singh, C.; Kumar, J.; Kumar, P.; Chauhan, B. S.; Tiwari, K. N.; Mishra, S. K.; Srikrishna, S.; Saini, R.; Nath, G.; Singh, J. Green Synthesis of Silver Nanoparticles Using

Aqueous Leaf Extract of *Premna Integrifolia* (L.) Rich in Polyphenols and Evaluation of Their Antioxidant, Antibacterial and Cytotoxic Activity. *Biotechnol. Biotechnol. Equip. 33* (1), 359–371. https://doi.org/10.1080/13102818.2019.1577699, **2019**.

[34] Ajitha, B.; Ashok Kumar Reddy, Y.; Sreedhara Reddy, P. Green Synthesis and Characterization of Silver Nanoparticles Using Lantana Camara Leaf Extract. *Mater. Sci. Eng. C*, *49*, 373–381. https://doi.org/10.1016/j.msec.2015.01.035, **2015**.

[35] Kumar, V.; Singh, D. K.; Mohan, S.; Hasan, S. H. Photo-Induced Biosynthesis of Silver Nanoparticles Using Aqueous Extract of Erigeron Bonariensis and Its Catalytic Activity against Acridine Orange. *J. Photochem. Photobiol. B*, *155*, 39–50. https://doi.org/10.1016/j.jphotobiol.2015.12.011, **2016**.

[36] Mostafa, Y. S.; Alamri, S. A.; Alrumman, S. A.; Hashem, M.; Baka, Z. A. Green Synthesis of Silver Nanoparticles Using Pomegranate and Orange Peel Extracts and Their Antifungal Activity against Alternaria Solani, the Causal Agent of Early Blight Disease of Tomato. *Plants*, *10* (11), 2363. https://doi.org/10.3390/plants10112363, **2021**.

[37] He, K.; Chen, N.; Wang, C.; Wei, L.; Chen, J. Method for Determining Crystal Grain Size by X-Ray Diffraction. *Cryst. Res. Technol*, *53* (2), 1700157. https://doi.org/10.1002/crat.201700157, **2018**.

[38] Adebayo-Tayo, B.; Salaam, A.; Ajibade, A. Green Synthesis of Silver Nanoparticle Using Oscillatoria Sp. Extract, Its Antibacterial, Antibiofilm Potential and Cytotoxicity Activity. *Heliyon*, *5* (10), e02502. https://doi.org/10.1016/j.heliyon.2019.e02502, **2019**.

[39] Sharma, D.; Ledwani, L.; Mehrotra, T.; Kumar, N.; Pervaiz, N.; Kumar, R. Biosynthesis of Hematite Nanoparticles Using Rheum Emodi and Their Antimicrobial and Anticancerous Effects in Vitro. *J. Photochem. Photobiol. B*, *206*, 111841. https://doi.org/10.1016/j.jphotobiol.2020.111841, **2020**.

[40]Philip, D. Honey Mediated Green Synthesis of Silver Nanoparticles. *Spectrochim. Acta. A. Mol. Biomol. Spectrosc*, *75* (3), 1078–1081. https://doi.org/10.1016/j.saa.2009.12.058, **2010**.

[41] Song, J. Y.; Kim, B. S. Biological Synthesis of Bimetallic Au/Ag Nanoparticles Using Persimmon (Diopyros Kaki) Leaf Extract. *Korean J. Chem. Eng*, *25* (4), 808–811. https://doi.org/10.1007/s11814-008-0133-z, **2008**.

[42] Srinithya, B.; Kumar, V. V.; Vadivel, V.; Pemaiah, B.; Anthony, S. P.; Muthuraman, M. S. Synthesis of Biofunctionalized AgNPs Using Medicinally Important Sida Cordifolia

Leaf Extract for Enhanced Antioxidant and Anticancer Activities. *Mater. Lett*, *170*, 101–104. https://doi.org/10.1016/j.matlet.2016.02.019, **2016**.

[43] Lü, J.; Lin, P. H.; Yao, Q.; Chen, C. Chemical and Molecular Mechanisms of Antioxidants: Experimental Approaches and Model Systems. *J. Cell. Mol. Med*, *14* (4), 840–860. https://doi.org/10.1111/j.1582-4934.2009.00897.x, **2010**.

[44] Javan Bakht Dalir, S.; Djahaniani, H.; Nabati, F.; Hekmati, M. Characterization and the Evaluation of Antimicrobial Activities of Silver Nanoparticles Biosynthesized from Carya Illinoinensis Leaf Extract. *Heliyon*, *6* (3), e03624. https://doi.org/10.1016/j.heliyon.2020.e03624, **2020**.

[45] Gautam, S. K.; Baid, Y.; Magar, P. T.; Binadi, T. R.; Regmi, B. Antimicrobial Study of Green Synthesized Silver Nanoparticles (AgNPs) by Using Ageratina Adenophora and Its Characterization. *Int. J. Appl. Sci. Biotechnol*, *9* (2), 128–132. https://doi.org/10.3126/ijasbt.v9i2.37822, **2021**.

[46] Gudikandula, K.; Charya Maringanti, S. Synthesis of Silver Nanoparticles by Chemical and Biological Methods and Their Antimicrobial Properties. *J. Exp. Nanosci*, *11* (9), 714–721. https://doi.org/10.1080/17458080.2016.1139196, **2016**.

[47] Elshikh, M.; Ahmed, S.; Funston, S.; Dunlop, P.; McGaw, M.; Marchant, R.; Banat, I. M. Resazurin-Based 96-Well Plate Microdilution Method for the Determination of Minimum Inhibitory Concentration of Biosurfactants. *Biotechnol. Lett*, *38* (6), 1015–1019. https://doi.org/10.1007/s10529-016-2079-2, **2016**.

[48] Shrestha, D. K.; Magar, A. B.; Pathak, I.; Parajuli, N.; Sharma, S.; Raj Sharma, K. Comparative Analysis of Biological Activities of Green-Synthesized Silver and Zinc Oxide Nanoparticles Using *Pogonatherum Crinitum* Extracts. *Arab. J. Chem*, *0*, 1–14. https://doi.org/10.25259/AJC_188_2024, **2025**.

[49] Hublikar, L. V.; Ganachari, S. V.; Patil, V. B.; Nandi, S.; Honnad, A. Anticancer Potential of Biologically Synthesized Silver Nanoparticles Using Lantana Camara Leaf Extract. *Prog. Biomater*, *12* (2), 155–169. https://doi.org/10.1007/s40204-023-00219-9, **2023**.

[50] Bhusari, S.; Sah, P. M.; Lakkakula, J.; Roy, A.; Raut, R.; Chondekar, R.; Alghamdi, S.; Almehmadi, M.; Allahyani, M.; Alsaiari, A. A.; Aljuaid, A.; Al-Abdullah, N. Green Synthesis of Silver Nanoparticles via *Taxus Wallichiana* Zucc. Plant-Derived Taxol: Novel Utilization as Anticancer, Antioxidant, Anti-Inflammation, and Antiurolithic Potential. *Green Process. Synth*, *12* (1), 20230051. https://doi.org/10.1515/gps-2023-0051, **2023.**